

FEDSM97-3103

PHASE-SEPARATED PIV MEASUREMENTS OF THE FLOW AROUND SYSTEMS OF BUBBLES RISING IN WATER

Lichuan Gui

Ralph Lindken

Wolfgang Merzkirch

Lehrstuhl für Strömungslehre
Universität Essen
D-45117 Essen , Germany

ABSTRACT

When measuring the flow structure in multiphase systems, as bubble column reactors, one aim is to measure the velocity distribution of all phases simultaneously e.g. by particle image velocimetry. A possible means for the separation of the signals originating from the different phases is the application of a digital mask technique. This technique that requires the existence of a significant difference in the size of the particles representing the two phases is described and then exemplified with a solid / liquid and a bubbly two-phase flow.

NOMENCLATURE

- D quadratic difference of PIV patterns
- D_A quadratic difference of continuous phase
- D_B quadratic difference of dispersed phase
- d_h hydraulic column diameter
- g_1 gray values of exposure 1
- g_2 gray values of exposure 2
- i discrete coordinate
- j discrete coordinate
- l bubble column length
- m displacement of interrogation window in x-direction
- m^* displacement of particle images in x-direction

- M number of pixels in x-direction
- n displacement of interrogation window in y-direction
- n^* displacement of particle images in y-direction
- N number of pixels in y-direction
- Δ total mask
- Δ_1 mask derived from exposure 1
- Δ_2 mask derived from exposure 2
- Δt time interval between exposures

INTRODUCTION

The flow induced by systems of gas bubbles rising vertically in a liquid is of particular interest for the design of bubble column reactors (see, e.g., Deckwer 1985). One may distinguish between two extreme situations expressed by the value of the ratio of the hydraulic column diameter, d_h , and the column length, l . At values $d_h/l \ll 1$, the flow is dominated by wall effects like in a two phase pipe flow. For values $d_h/l \approx 1$ the bubbles rise in a nearly undisturbed environment. The liquid which is the continuous phase in this two-phase system may have a mean velocity component in or against the direction of the bubble rise velocity. The possible mass exchange between the gaseous and the liquid phase is strongly influenced by the distribution of the bubbles and by the relative flow and turbulence induced by the bubbles in the liquid. This relative flow develops from the turbulent wakes left behind by the bubbles. Another quantity of interest for the mass exchange is the contact time between the two phases. This quantity depends on the geometrical dimensions of the column and on

the bubbles' rise velocity. Analytical solutions are known for the rise velocity of a single bubble. But it is also known that the rise velocity of swarms or systems of bubbles can be up to twice the value for a single bubble, because these bubbles rise in the wake produced by the preceding bubbles in the system (Tassin and Nikitopoulos 1995).

In order to model the fluid mechanical processes in such bubble reactors, experimental data on the relative flow between the two phases and its turbulent structure are needed. Measurements on a variety of two-phase flows with dispersed gaseous phase have been performed with hot-wire anemometry (Wang et al. 1987), laser Doppler anemometry (Vassalo et al. 1993) and particle image velocimetry (Hassan et al. 1992), just to mention a few characteristic approaches. Since the relative flow field induced by rising bubbles is highly unsteady, an optical whole-field technique like particle image velocimetry (PIV) appears particularly appropriate for such studies. In a PIV recording the signals indicating the velocities of two phases (bubbles / water seeded with tracer particles) are received simultaneously, and special technical means are required for separating these signals, if a difference in the velocities of the two phases is present, like in the cases considered here. This separation can be realized by using fluorescent tracer particles (Hassan et al. 1993; Hilgers et al. 1995; Sridhar and Katz 1995), or by making use of the fact that a significant difference in the size of the particles representing the two phases (bubbles/tracers) exists (Gui and Merzkirch 1996). In this paper we report on experience made with applying the latter technique that uses a digital phase mask for studying the two-phase flow with relatively large solid and gaseous particles dispersed in water. The experiments are performed in a water tank for which the ratio d_h/l assumes a value of approximately one.

DIGITAL MASK TECHNIQUE FOR PHASE SEPARATED VELOCITY MEASUREMENTS WITH PIV

We are using two different ways to record PIV events for the determination of the velocity distribution of the two phases. One way consists of taking two single exposures with two synchronized CCD-cameras at a defined time interval as described by Merzkirch and Wagner (1996). Both cameras are directed on an identical area of the flow field. Differences in the optical way are eliminated by a calibration procedure. The second way is to use only one CCD-camera, which allows taking two single exposures in a defined time interval by storing the first picture in the non-light sensitive part of the pixels. In both cases we obtain two consecutive single exposures at a time interval adapted to the actual flow conditions.

The PIV recordings are evaluated by the Minimum Quadratic Difference (MQD) method described by Gui and Merzkirch (1996). The MQD-method is based on the search of the minimum of the quadratic difference of two particle ensembles.

$$D(m,n) = \frac{1}{MN} \sum_{i=1}^M \sum_{j=1}^N [g_1(i,j) - g_2(i+m,j+n)]^2 \quad (1)$$

where g_1 and g_2 are the grey values of the pixels in a $N \times M$ window in exposures (1) and (2).

The MQD method is a tracking algorithm, based on the principle of minimizing the (quadratic) differences between multi-component vectors or matrices (least square) in order to investigate the degree of similarity existing between such quantities, thus allowing application of particle tracking to highly seeded flow. The use of the mask technique in combination with the MQD-method is not a restriction of the applicability of this technique. The mask technique can be combined with any other search algorithm.

We assume that phase A is dispersed in a continuous phase B. The signals resulting from the two phases are separated by a mask $\Delta(i,j)$ superimposed to the window, such that

$$\Delta(i,j) = \begin{cases} 0 & \text{if pixel } (i,j) \text{ belongs to phase A} \\ 1 & \text{if pixel } (i,j) \text{ belongs to phase B} \end{cases} \quad (2)$$

A threshold value for the particle image size, following from experience and knowledge of the experimental conditions, assigns the signals to either phase A or B.

Mask for the evaluation of the velocity distribution of the dispersed phase

The continuous phase B is covered by the mask for determining the velocity of the dispersed phase A. The mask $\Delta_1(i,j)$ is superimposed on the grey value distribution of only the first exposure g_1 in equation (1):

$$D_A(m,n) = \frac{\sum_{i=1}^M \sum_{j=1}^N [g_1(i,j) - g_2(i+m,j+n)]^2 [1 - \Delta_1(i,j)]}{\sum_{i=1}^M \sum_{j=1}^N [1 - \Delta_1(i,j)]} \quad (3)$$

While equation (1) refers to the tracking of all particle images, equation (3) describes only the tracking of images of particles attributed to phase A.

Figure (1) explains the mask technique with numerically simulated PIV pictures. The ensembles in figure (1.a) are separated by a time interval Δt . In both pictures we have a great number of small tracer images (phase B) and two big

images of the dispersed phase A. A quadratic window is chosen in the first exposure (left). The evaluation of the

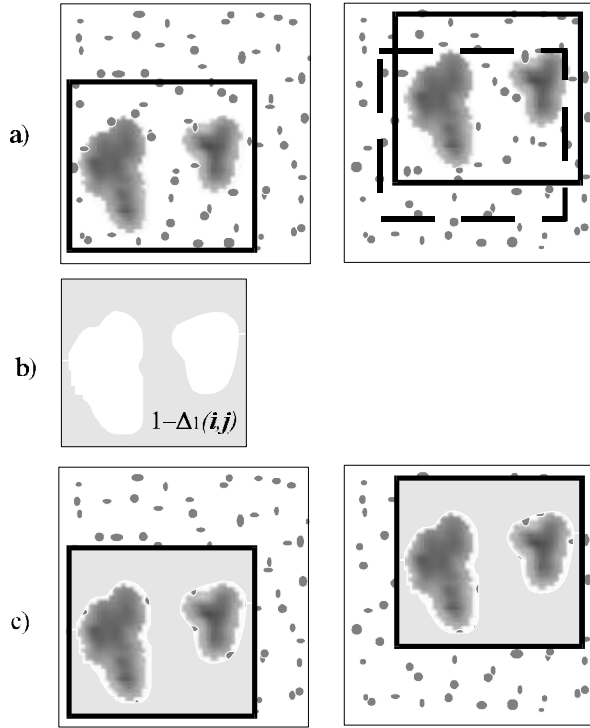


Fig.1: Simulated PIV recordings of a two-phase flow with small tracer particle images and images of the big dispersed particles.
a) Two consecutive exposures (left, right) separated by time interval Δt . A quadratic interrogation pattern (or window) is chosen for the evaluation.
b) Shape of the mask for obscuring the small tracer particle images.
c) Measurement of the displacement of the dispersed particles with the mask applied to the quadratic interrogation pattern.

unmasked exposures in figure (1.a) is dominated by the images of the two big particles.

But the trajectories of the small particles moving at a velocity different from that of the dispersed phase are adding noise. The velocity of the whole (unmasked) window is different from the velocity of the dispersed particles. By applying the digital mask shown in figure (1.b) the images of the tracer particles, except for some particles close to the big image are covered and the noise is reduced considerably.

Mask for the evaluation of the velocity distribution of the continuous phase

For determining the velocity of the continuous phase we apply a different version of the mask technique (Fig.2). Again

a square window is chosen and the images of the dispersed phase are masked in exposure (1) by the mask $\Delta_1(i,j)$, which is only one part of the total mask Δ . The position of the window

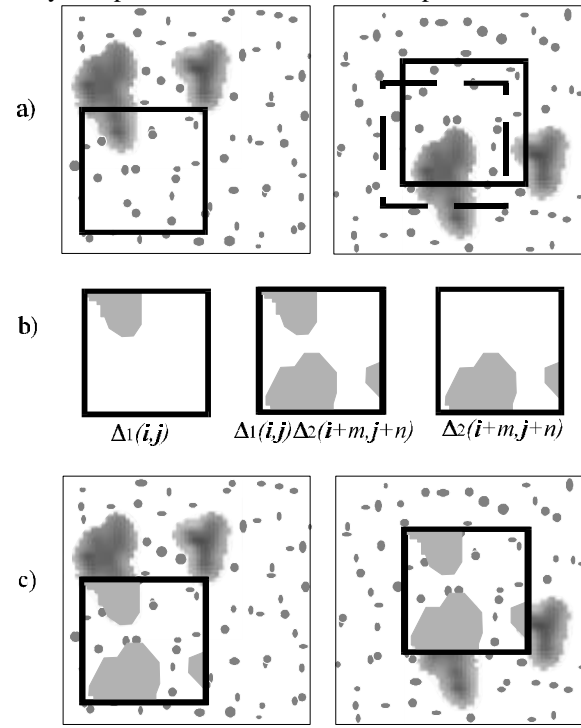


Fig. 2: The same simulated recordings as in Fig. 1.
a) Application of the quadratic interrogation pattern to the unmasked first exposure (left) and variable position of the pattern in the second exposure (right).
b) Definition of the total mask (middle) composed of Δ_1 (left) and the variable mask $\Delta_2(i+m,j+n)$ (right).
c) Application of the total mask obscuring the dispersed particle images for measuring the displacement of the tracer particle images.

in the second exposure is varied like in figure (1), but in addition a variable mask $\Delta_2(i+m,j+n)$, redefined for every position (m,n) , is obscuring the dispersed particle images in the second exposure. The total mask

$$\Delta = \Delta_1(i, j) \cdot \Delta_2(i + m, j + n) \quad (4)$$

applies to the particle images of phase A in the first and in the second exposure.

The minimum of D_B is determined for the tracer particle image pattern in the unmasked areas as shown in figure (2.c).

Combining the mask Δ as in equation (4) with the minimum quadratic difference yields

$$D_B(m,n) = \frac{\sum_{i=1}^M \sum_{j=1}^N [g_1(i,j) - g_2(i+m,j+n)]^2 \Delta_1(i,j) \Delta_2(i+m,j+n)}{\sum_{i=1}^M \sum_{j=1}^N \Delta_1(i,j) \Delta_2(i+m,j+n)} \quad (5)$$

The displacements (m_A^*, n_A^*) or (m_B^*, n_B^*) experienced during the time interval Δt are obtained by comparing the results from equation (3) or equation (5):

$$D(m^*, n^*) = \min \{D(m, n)\} \quad (6)$$

The position assigned to the displacement of each phase has to be evaluated separately as the centre of gravity of each particle image (phase A) or the pattern of particles (phase B).

TEST CASE: LIQUID / SOLID TWO PHASE FLOW

As a first test case we choose a solid-fluid flow. This has the advantage, that the size and shape as well as the intensity of the reflections from the dispersed phase are relatively uniform compared to bubbly flow. The shadows produced by the dispersed particles, caused by laser light incident from just one side, disturb the illumination of the tracer particles „behind“ the dispersed phase in a more predictable way.

Figure (3.a) shows two consecutive single exposures at a time interval $\Delta t = 20$ ms. From the figure it is obvious, that the

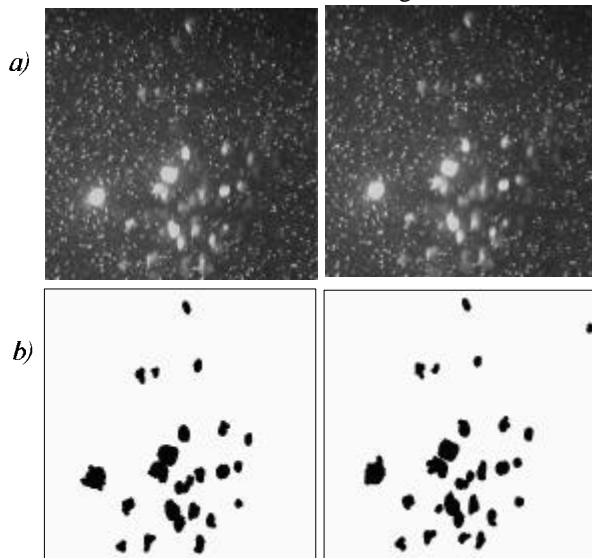


Fig.3: a) Two consecutive digital recordings showing the distributions of small tracer particles and big dispersed buoyant particles in a water tank. Field of

view is 450×450 pixels = 9×9 cm². Time interval between exposures is $\Delta t = 20$ ms.

b) Application of the mask for separating the regimes of phase A and phase B

white speckles can be assigned to two groups. The size of the images of the tracer particles (phase B) is in the order of 5 to 20 pixels. The seed concentration is of the order of 100 to 300 particles per cm³. The big white speckles are significantly larger than 30 pixels, making 30 pixel an adequate threshold value for phase discrimination.

The phase mask for separation of phase A (black area) and phase B (white area) in figure (3.b) allows the determination of the velocity distributions in figure (3.a).

Figure (4) presents the results of the evaluation with the MQD method as a vector plot. The origins of the resulting vectors in figure (4) are the centers of gravity of the respective phases in the first exposure as discussed by Gui and Merzkirch (1996). The 450×450 pixel exposures in figure (3) offer more than 700 velocity informations of the continuous phase by MQD-particle tracking and one velocity vector for each dispersed particle detected. The vectors referring to the two phases can be distinguished by their size. The higher velocity of the buoyant dispersed phase is evident. For a more detailed description of the flow around the particle a higher seeding rate is necessary.

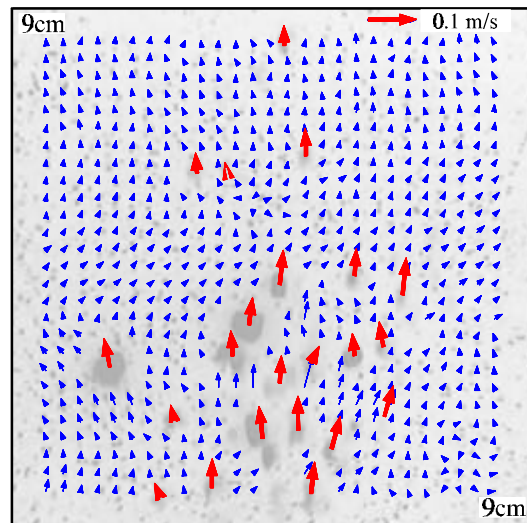


Fig. 4: Result of the velocity measurement for the experimental patterns shown in Fig. 3. The indicated reference velocity is 0.1 m/s. The velocities of the continuous and dispersed phase can be distinguished by the size of the vectors.

TEST CASE: BUBBLY TWO PHASE FLOW

The application of the phase mask to a system of air bubbles rising in water is exemplified in Figure (5). The two consecutive digital recordings presenting a field of view of $102 \times 102 \text{ mm}^2$ (512×512 pixels) are separated by a time interval

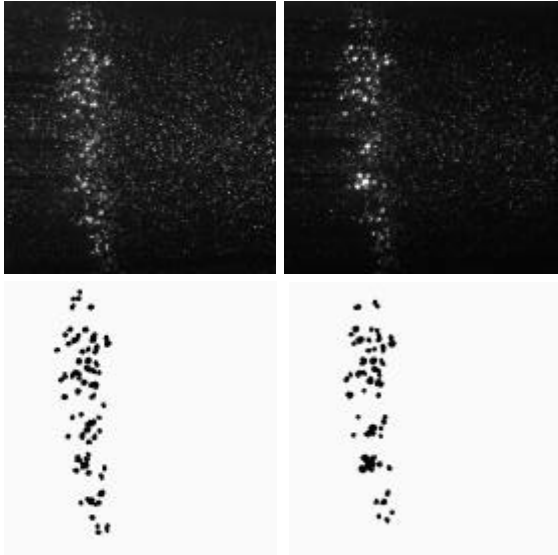


Fig. 5: a) Two consecutive digital recordings showing the distributions of small tracer particles and dispersed bubbles in a bubble column reactor. Field of view is 512×512 pixels = $10,2 \times 10,2 \text{ cm}^2$. Time interval between exposures is $\Delta t = 10 \text{ ms}$.
b) Application of the mask for separating the regimes of phase A and phase B

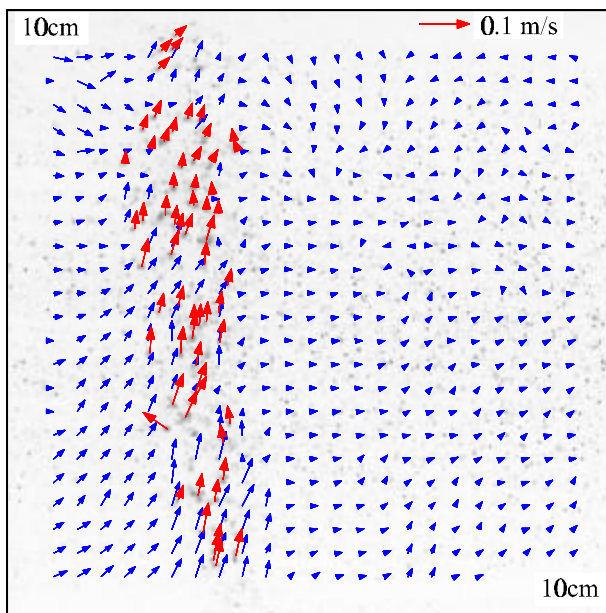


Fig. 6: Result of the velocity measurement for the experimental patterns shown in Fig. 5. The indicated reference velocity is 0.1 m/s. The velocities of the continuous and dispersed phase can be distinguished by the size of the vectors.

of 10 ms. The bubble size is in the range of 1 to 3 mm in diameter. The projected areas of the bubbles in the image plane are larger than 20 pixels. The masks applied to the dispersed phase A are shown in Figure (5.b). We used a threshold value of 20 pixels. The velocity of the rising bubbles can be clearly determined (Fig. 6). While the chosen size of the field of view is big enough for giving a survey of the whole flow process, the digital resolution is too low for allowing details of the flow of the continuous phase being resolved. Entrainment of the water by the stream of rising bubbles is visible only in the immediate neighbourhood of bubbles (Fig. 6). Another reason for not resolving the induced water velocity with a sufficient accuracy in this case is the dynamic range of the PIV measurement, here determined by the chosen time interval of 10 ms.

SUMMARY

The described digital mask technique is suitable for separating the signals originating from the different phases in a two-phase flow. The mask relies on the existence of a significant difference in size of the particles representing the two phases, here: small tracer particles and bigger dispersed particles. Application of the mask is demonstrated with a few test cases. In current experiments the mask is used for investigating the near field around groups of bubbles rising vertically in water (see also oral presentation of this paper)

ACKNOWLEDGMENT

This research is supported by Deutsche Forschungsgemeinschaft (DFG Az. Me 484/32).

REFERENCES

- Deckwer, W.-D., 1985, "Reaktionstechnik in Blasensäulen," Salle+Sauerländer Verlag, Frankfurt/Aarau, Germany.
- Gui, L., and Merzkirch, W., 1996, "A method of tracking ensembles of particle images," *Experiments in Fluids*, Vol. 21, 465-468.
- Gui, L., and Merzkirch, W., 1996, "Phase-separation of PIV measurements in two-phase flow by applying a digital mask technique," *ERCOFTAC Bulletin*, Vol. 30, 45-48.
- Hassan, Y.A., Blanchat, T.K., Seeley, Jr., C.H., and Canaan, R.E., 1992, "Simultaneous velocity measurements of both components of a two-phase flow using particles image velocimetry," *International Journal of Multiphase Flow*, Vol. 18, 371-395.
- Hassan, Y.A., Philip, O.G., and Schmidl, W.D., 1993, "Bubble collapse velocity measurements using a particle image velocimetry technique with fluorescent tracers," *ASME-FED*, Vol. 172, 85-92.

- Hilgers, S., Merzkirch, W., and Wagner, T., 1995, "PIV measurements in multiphase flow using CCD- and Photo-camera," *ASME-FED*, Vol. 209, 151-154.
- Merzkirch, W., and Wagner, T., 1996, "PIV with two synchronized video cameras," *IMEchE Conference Transactions*, 237-242.
- Sridhar, G., and Katz, J., 1995, "Drag and lift forces on microscopic bubbles entrained by a vortex," *Physics of Fluids*, Vol. 7, 389-399.
- Tassin, A.L., and Nikitropoulos, D.E., 1995, "Non-intrusive measurements of bubble size and velocity," *Experiments in Fluids*, Vol. 19, 121-132.
- Vassallo, P.F., Trabold, T.A., Moore, W.E., and Kirouac, G.J., 1993, "Measurement of velocities in gas-liquid two-phase flow using laser Doppler velocimetry," *Experiments in Fluids*, Vol. 15, 227-230.
- Wang, S., Lee, S.J., Jones, Jr., O.C., and Lahey, Jr., R.T., 1987, "3-D turbulence structure and phase distribution measurements in bubbly two-phase flow," *International Journal of Multiphase Flow*, Vol. 13, 327-343.